M-FISH analysis shows that complex chromosome aberrations induced by α-particle tracks are cumulative products of localised rearrangements

Rhona M. Anderson ‡, David L. Stevens and Dudley T. Goodhead

MRC Radiation and Genome Stability Unit, Harwell, Didcot,

Oxfordshire. OX11 0RD. UK.

‡To whom correspondence should be addressed to:
Rhona M. Anderson
MRC Radiation and Genome Stability Unit
Harwell
Didcot
Oxfordshire
OX11 0RD
UK
Tel: 01235 834393
Fax: 01235 834776
e-mail: (r.anderson@har.mrc.ac.uk)

Manuscript classification	Major: Biological Sciences Minor: Biophysics		
Manuscript Information	Number of text pages	=	17
	Number of figures	=	4
	Number of tables	=	1
	Number of supplementary appendix pages	=	3
	Number of supplementary figures	=	1
	Number of supplementary tables	=	1

Complex chromosome aberrations are characteristically induced after exposure to low doses of densely ionising radiation, but little is understood about their formation. To address this, we irradiated human peripheral blood lymphocytes (PBL) *in vitro* with 0.5 Gy densely ionising α-particles (mean of 1 α-particle/cell) and analysed the chromosome aberrations produced using 24-colour M-FISH. Our data suggest that complex formation is a consequence of direct nuclear α-particle traversal and show that the likely product of illegitimate repair of damage from a single α-particle is a single complex exchange. From an assessment of the 'cycle structure' of each complex exchange we predict α-particle-induced damage to be repaired at specific localised sites, and complexes to be formed as cumulative products of this repair.

Ionising radiation is extremely effective in producing chromosomal aberrations. Practically, this enables their induction to be applied in the study of assessing cancer risks and other public health questions associated with the environment, including as specific biomarkers of exposure (1) (2), or from occupational (3) and therapy-related exposures (4). Double-strand breaks (dsb) of varying complexity are an important class of damage induced after exposure to ionising radiation and chromosome aberrations are formed as one consequence of the cellular processes initiated for their repair (5-8). However, the dynamics of aberration formation are not known. One approach that allows mechanistic questions to be addressed is to characterise the different types of chromosome aberration induced after exposure to specific qualities of ionising radiation. Each radiation-induced damaged cell will contain a unique rearrangement, but it is expected that the qualitative 'form' of the induced rearrangement will reflect the initial spectrum of dsb damage induced. Assuming that the damage induced is a direct consequence of the radiation track interacting with the DNA, then the structure of the radiation track should influence the type of chromosome aberration observed (2, 9, 10). Collectively from this, predictions can be made as to how damaged chromatin 'ends' associate prior to their ultimate mis-repair.

The range and dimensions of a 5 MeV α-particle, like that emitted from radon in the environment, are typically short (40 μm) and of limited maximum radial spread (0.1 μm) with ~90% of energy deposition within 10 nm. Consequently, high-linear energy transfer (LET) α-particles are only capable of intersecting a very small fraction of the total cell volume, which if by chance is intersected, will almost never be intersected by another track (10). These particles are however extremely effective in producing a high density of

localised molecular lesions due to the deposition of large clusters of energy (400-800eV) along the whole length of the track (~25-50 such clusters in nucleosomes per cell per α-track). These energy depositions are capable of inducing complex local damage to the chromatin (1 or more dsb, base damage and other associated breaks) that is known to repair less efficiently than simple dsb (11). By comparison, cellular exposure to low-LET radiation, such as X-rays, results in an energy distribution that is spread more uniformly through the cell with more minor clustering. So, the spatial patterns of energy distribution by high- and low-LET radiations are characteristically different over cellular, subcellular and macromolecular distances (12).

Complex chromosome aberrations (defined as involving 3 or more breaks in 2 or more chromosomes) (13) are known to be characteristically induced after exposure to low doses of high-LET radiation (1, 14-18). To date, the full cytogenetic complexity of these aberrations has not been revealed because standard fluorescence *in situ* hybridisation (FISH) techniques are limited in the number of chromosomes that can be 'painted'. The development of multiplex-FISH (M-FISH) (19) however has changed this because it enables the discrimination of all the human chromosomes via the combinatorial labelling of individual chromosomes with spectrally distinct fluorophores. With the exception of interchanges between homologues, it allows all the chromosomes participating in each aberration, within any cell, to be observed and the relationship between different aberrant chromosomes to be determined (20). We have used this technique to examine the cellular-wide damage and complexity of induced aberrations after exposure to a low-dose of high-LET α-particles (1), using a relatively high dose of low-LET X-rays as a

reference, with the aim of addressing the question of how α-particle-induced complex chromosome aberrations are formed.

MATERIALS AND METHODS

Cell Culture and *in vitro* irradiation. Whole blood was collected from three healthy volunteers and separated to isolate the lymphocyte (PBL) fraction using vacutainer-CPT mononuclear cell preparation tubes (Becton Dickinson, Oxford, UK). The cells were plated as a monolayer and irradiated in G_0 with either 0.5 Gy α-particles (3.26 MeV) or 3 Gy X-rays (250 kV) (1). The α-particle dose was chosen to give on average 1 α-particle traversal per cell and the X-ray dose was selected at a much higher level to ensure that sufficient complex aberrations were induced for comparative purposes (21). After irradiation, T-lymphocytes were stimulated to divide and harvested to obtain 1st division metaphase chromosomes as previously described (1).

Multiplex *in situ* hybridisation (M-FISH). Fresh slides of metaphase chromosomes were hardened (3:1 methanol : acetic acid for 1 h, dehydrated, baked at 65^{o}C for 20 min then 10 min in acetone) and pre-treated with RNAse (100μg/ml) at 37^{o}C for 1 h. After washing in 2xSSC and PBS, the cells were treated with 0.65M KCL for 10 min at room temperature, washed, dehydrated and further treated with 0.16 μg/ml Proteinase K in Tris HCL/$CaCl_2$ for 10-30 min at 37^{o}C. Finally, the cells were washed, fixed in 4% paraformaldehyde for 5-10 min, washed again and dehydrated. For hybridisation, cells were denatured in 70% formamide/2xSSC at 72^{o}C for 3 min and dehydrated for 1 min each in 70/90/100% ethanol. Parallel to this, the commercially available 24-colour paint

cocktail SpectraVision™ Assay, Vysis (UK) Ltd), was denatured (73°C for 6 min). Cells were left to hybridise for 36-48 h at 37°C before being washed in 0.4xSSC/0.3% Igepal (Sigma, UK) (71°C for 1.5 min) and 2xSSC/0.1% Igepal (room temperature for 10 sec). Cells were counterstained using DAPI III, sealed and stored in the dark at –20°C.

Metaphase chromosomes were visualised using a 6-position Olympus BX51 fluorescent microscope containing individual filter sets for each component fluor of the SpectraVision (Vysis (UK) Ltd) probe cocktail plus DAPI (Spectrum Gold, Spectrum Far-red, Spectrum Aqua, Spectrum Red and Spectrum Green). Digital images were captured for M-FISH using a charged-coupled device (CCD) camera (Photometrics Sensys CCD) coupled to and driven by Genus (Applied Imaging, UK). In the first instance, cells were karyotyped and analysed by enhanced DAPI banding. Detailed paint analysis was then performed by assessing paint coverage for each individual fluor down the length of each individual chromosome, using both the raw and processed images for each fluor channel. A cell was classified as being apparently normal if all 46 chromosomes were observed by this process, and subsequently confirmed by the Genus M-FISH assignment, to have their appropriate combinatorial paint composition down their entire length.

Chromosome aberration classification. Exchange aberrations involving three or more breaks in two or more chromosomes were classified as *complex* and assigned the most conservative C/A/B (minimum number of Chromosomes/Arms/Breaks involved) (13). To do this, the relative breakpoint positions of the visible colour junctions (Fig. 1A) were estimated using enhanced DAPI banding and an assessment of arm ratio and size of rearranged material. Using coloured markers, a cartoon detailing the position of these

'reactive breaks' prior to their complex interaction, was produced (Fig. 1B). Then, assuming each breakpoint produces two 'free-ends', the observed complex was reconstructed using this cartoon until all the 'free-ends' were 'closed' (Fig. 1C-E) (Personal communication, JRK Savage). In other words, all the break-ends have a partner and all rearranged chromosomes have telomeric ends, unless they are ring chromosomes; for detailed discussion see (22). When more than one option to achieve completeness was possible, the rearrangement that produced the minimum C/A/B was used. Missing or unresolvable elements required to achieve completeness were easily identified by this procedure and as a consequence, could be assumed. (23).

Complex exchanges were thus grouped as complete, unresolved incomplete or true incomplete exchanges. Each complex exchange was then categorised as a single event and independent of any other complex, *simple* (maximum of two breaks in two chromosomes) or *break* (chromosome breaks not involving additional chromosomes) observed in the same cell.

Sequential exchange complexes (SEC). A SEC is defined as a complex exchange that can be reduced into smaller independent exchange events (cycles) that are temporally or spatially separated from one another, but where each event has a common link (24) (for detailed discussion see (22)). Characterised by a nomenclature system introduced by Sachs *et al*., (1999) (25), each 'cycle' gives information on the minimum number of interactions (and therefore free-ends) that were proximate, and as a consequence, the minimum number of chromatin strands that mis-repaired within the repair site volume.

For many complex aberrations, there may be a number of possible 'rejoining cycles' that are theoretically capable of reconstructing the observed complex (for detailed

discussion see (22)). Therefore in an effort to standardise this data, we assigned the most conservative, or obligate cycle structure (22), to each complex (Fig. 1E). Since mechanistic interpretations were performed using these obligate cycle structures, it should be highlighted that the obligate cycle structures may not represent the actual route of formation of each complex.

Therefore this classification identifies those complexes that can be reduced into SEC and the recorded obligate cycle structure represents the minimum degree of complexity required to form each complex exchange.

Simulation. This simulation, developed to estimate the number of chromosomes crossed by a α-particle track in a G_0 cell nucleus, relies on the observation that any chord passing through a sphere lies on an equatorial plane. By modeling the number, areas and shapes of the intersections of chromosome domains with representative nuclear equatorial planes (NEPs), and with appropriate weighting, a reasonable representation of the interaction of α-particles with spherical nuclei can be obtained. The simulation uses no adjustable parameters and it assumes only that the cell nucleus is spherical, valid for human lymphocytes, and that there are 46 equally sized chromosome domains closely packed within the nucleus. The method could be adapted to any nucleus shape with axial symmetry, but is limited to radiations producing linear and narrow tracks.

If a chromosome domain is assumed to be spherical and it intersects randomly with a NEP (Fig. 2), its area of its intersection can be assumed to be $\pi(r^2-x^2)$, where r is the domain radius and x is chosen from a uniform random distribution between -r and r. Domain areas were sequentially subtracted from the NEP area until the calculated domain area was larger than the residual area of the NEP. The last domain area was then taken as

that residual area. By repeating this process 200 times we obtain information on the number and areas of chromosome domains intersecting NEPs. The number of chromosome domains intersecting with NEPs is shown in (Fig. 3A).

Representative NEPs from this distribution were constructed with domain areas drawn by hand as circular as possible whilst ensuring efficient packing (e.g. Fig 4A). Nineteen parallel chords were then placed uniformly across each NEP (Fig. 5A) and the number of domains crossed by each chord was recorded. By weighting the number of domains crossed by a chord, by the likelihood that a chord of that length will occur through a spherical nucleus (proportional to area of the circular element, eg. illustrated for two areas in Fig. 5B), a distribution of the number of domains a chord/track will cross was obtained. The means of the distributions are shown in Fig. 3B. By weighting these distributions with the likelihood that they will occur (Fig. 3A) the overall distribution of the number of domains α-particles will cross, was obtained (Fig. 6A). Also shown in Fig. 6A is the distribution after adjustment for involvement of homologous chromosomes (see legend.

RESULTS AND DISCUSSION

Quality of aberration induced by nuclear traversal of one α-particle. Under the experimental conditions used here, each human peripheral blood lymphocyte (PBL) irradiated with 0.5 Gy α–particles and 3 Gy X-rays, would receive on average 1 and ~700 tracks respectively, with the X-rays causing about 6-fold more ionisations (Figs. 4A and B). Interestingly though, we observed no difference in the total cellular damage,

based on the mean number of damaged chromosomes (C) and breaks (B) involved, between the two radiation qualities (low dose α-particles: C = 5.37±0.33, B = 7.36±0.47 and high-dose X-rays: C = 5.29±0.46, B = 6.90±0.6). Instead the spatial differences in deposition of energy were reflected by the quality of aberration classified. Specifically, 83% of total exchanges detected were complex (3 or more breaks in 2 or more chromosomes) after α-particles (Fig. 7). This compares with only 36% after the high dose of X-rays and is consistent with the observations of Loucas and Cornforth (2001) (23). More striking, 87% of all cells observed to be damaged after α-irradiation contained at least 1 fully definable complex rearrangement (Fig. 7), suggesting that the damage from α-particle traversal nearly always repairs as a complex exchange event. In addition, the complexity of each complex was greater and the mean number of independent exchanges/cell fewer, after 0.5Gy α-particles compared to the relatively high dose of 3Gy X-rays. Therefore radiation track structure does determine the 'forms', as well as the total yield, of aberration induced (10, 11, 26), supporting the view that spatial proximity between induced dsb influences the chance of their interaction (27).

We used a novel co-irradiation system to assess whether complex aberrations might also arise in cells that had not been directly traversed by a α-particle track. Our data show that complexes were induced only in cells in the irradiated sub-population, confirming their induction to be dependent upon α-particle nuclear traversal (Supplementary information on the Web).

We next asked whether each complex was the end-product of the interaction of damage caused by more than 1 α-particle traversal. To do this we independently developed a model that predicted the distribution of the number of chromosome domains that would

be traversed by a α-particle, given random trajectories through the G_0 cell nucleus (Figs. 2, 3 and 5). Comparison of this theoretical distribution with the distribution of the number of chromosomes experimentally observed in each complex suggests that the damage induced by the nuclear traversal of a single α-particle results in the formation of a single complex exchange (Fig. 6A). Considering this argument with the fact that a number of PBL will be traversed by more than 1 α-particle, a statistical consequence of broad-beam exposure, we categorised each aberration classified as either a simple, complex or break, as an independent event. From this, we can show a similar trend between the Poisson distribution of cells hit by 1, 2, 3 or 4 α-particles and the number of independent events observed in each damaged cell (Fig. 6B). Consequently, we propose that the damage arising from 1 α-particle will normally result in 1 complex event. If so, then this is relevant for the study of single track or low dose cellular effects and it could also have major implications for epidemiological studies assessing public health risks from the exposure to domestic radon. It is also relevant to note that this predominant induction of complex chromosome aberrations throughout a population of PBL after exposure to an environmentally relevant dose of α-particles, strengthens the authors' proposal that complexes *per se* could be exploited as biomarkers for the identification of highly exposed individuals (1). Work focussing on defining a more detailed 'biomarker profile' is on going.

Formation of α-particle-induced complex aberrations. It is generally accepted that radiation-induced dsb formed in G_0/G_1 are repaired by the non-homologous end-joining (NHEJ) pathway (28); the role of homologous recombination (HR) and the recruitment of homologous chromosomes (29) in complex aberration formation is not known.

Considering α-particle-induced complexes, we found 13 out of 56 damaged cells had at least one complex that involved at least 1 homologous chromosome pair (Table 1C) and overall, ~1/3 of all damaged cells contained at least one damaged pair (Table 1B and 1C). To determine whether this represented homologous pair non-random involvement in these α-particle-induced complexes, a Monte Carlo simulation of 1,000,000 tests was performed. The results show that the observed level of homologous pair involvement in complex exchanges did not represent a deviation from that expected by a random breakage and reunion model and is consistent with the prediction that a significant proportion of exchanges will involve both homologues (22). Damage to homologous chromosome pairs can however limit their discrimination into separate independent complex events, with the result that it is not possible to determine whether those particularly complex events are products of damage caused by the traversal of >1 α-particle (Table 1B and C). Consequently, the data were sub-divided into Table 1A-C, with all analyses performed using only the 'A' sub-set (damaged metaphases not involving two damaged homologues).

Based on our theoretical model (Fig. 6A), we predict that the nuclear traversal of a single α-particle will intersect with between 1 and 8 different chromosome domains and therefore, the complexity of any observed α-particle-induced complex should not involve more than 8 different chromosomes. Our experimental data show complexity to range from involving 2 chromosomes and 3 breaks to 7 chromosomes and 10 breaks with the average involving 4 different chromosomes and 6 different breaks (Table 1A). Chromosomes are known to occupy discrete territories or domains during interphase (30) and it is expected that there is limited intermingling of chromatin strands, yet the

complexity of a α-particle-induced complex suggests multiple damaged chromatin strands must associate. Therefore, by what mechanism do damaged chromatin strands from multiple domains repair allowing the resulting product to be visible as a single complex event? To address this, we derived every possible theoretical 'rejoining path' of all damaged chromosome 'ends' that could have resulted in the generation of each α-particle-induced complex that was visualised by M-FISH (see Materials and Methods, (Fig. 1) and further detailed in (22, 23, 25). Specifically, we asked whether a complex could be the end product of a number of smaller events that occurred at different sites involving common chromosomes.

Using the complexes from Table 1A only, we found 23/42 were of the non-reducible complex type but that 19/42 could be reduced into smaller sequential exchanges (SEC) (see Materials and Methods). Interestingly, two complexes could only be 'reconstructed' into the observed complex as SECs ie. it was not theoretically possible to produce the complex as one large non-reducible cycle. For the remaining SEC, each complex could be 'reconstructed' either as one large cycle or via the potentially numerous combinations of theoretically possible cycles.

The cycle sizes necessary to result in the formation of the 'non-reducible' complexes ranged from c2 to c6, implying that up to 6 different breaks (12 free-ends) were illegitimately repaired within the same nuclear area. It is known that densely ionising α-particles are capable of inducing multiple sites of DNA damage in a localised volume (26), thus key to the formation of these cycles are questions that relate to the organisation of chromatin at the time of damage (31, 32). In other words, are breaks induced in chromatin loops of pre-existing functional associations, or do damaged 'ends' mobilise to

form ‘chromatin aggregates’ that function as ‘repair centres’? (30, 33-35). Comprehensive statistical analysis of our data (not shown) show the distribution of breakpoints for each chromosome to be essentially random, with no evidence of association between chromosomes involved in each complex (analysis based on Table 1A). Thus we could not relate chromosome involvement within each complex to chromosome territory organisation in interphase. Recognising the infinite number of possible trajectories of a α-particle track through a cell nucleus, and that both repair centres and pre-existing associations localise within inter-chromatin spaces, we propose our data are more consistent with the moving together of chromatin-ends after damage. We believe it seems unlikely that all breaks occurred at one site, based on considering the dimensions of the α-particle track and the number of different chromosomes involved in each complex: this would require chromatin associations to occur at high density, however dynamic, and typically to involve many different chromatin loops. Instead, we predict that limited directed movement to the nearest local repair centre could account for proximity effects (27) and also, the observed number of different chromatin strands involved in each cycle. To elaborate on this latter point, 25/42 of the α-particle-induced complexes were reducible into SEC’s; Table 1A shows the obligate SEC for each. This obligate structure represents the minimum number of chromatin break-ends in each cycle that would be required to form that particular complex, but is not necessarily the most likely (Fig. 8 A, B and C) (22). For many SEC’s, theory predicts other possible combinations of rejoining cycles, each of which involve many more chromatin strands in each cycle and that, by definition, would be required to be in the same space for repair. Therefore it cannot be excluded from these data that the complexity of each α-particle-

induced complex is due to the recruitment of undamaged DNA (36) consistent with Chadwick and Leenhouts (37) theory that damaged and undamaged DNA interact to form exchanges.

The damage induced by the traversal of a α-particle is expected to result in the formation of numerous 'hidden' intra-chromosome rearrangements; their formation should however follow the same scheme. Specifically, our data are consistent with each theoretical rejoining cycle, for each observed complex, representing a single inter-chromatin space that was intersected by a single α-particle track (30). These spaces form lacunas that both separate chromosome domains and invaginate within domains, and into which chromatin loops may extend. Assuming that an inter-exchange will only occur at boundary zones of chromosomal domains (38), then the number of individual cycles making up each complex should reflect the number of chromosome-chromosome domain boundaries damaged. Common chromosome domains, but different inter-chromatin spaces will then result in the cumulative generation of the observed complex.

In conclusion, we propose that α-particle-induced complex chromosome aberrations arise as products of illegitimate repair of damage induced directly in chromatin loops, with repair most likely occurring after limited movement to the nearest local 'repair factory'. Provided two or more domains are intersected by a α-particle, the most likely outcome of repair will be the cumulative build-up of a complex chromosome aberration.

1. Anderson, R. M., Marsden, S. J., Wright, E. G., Kadhim, M. A., Goodhead, D. T. & Griffin, C. S. (2000) *Int J Radiat Biol* **76,** 31-42.
2. Deng, W., Morrison, D. P., Gale, K. L. & Lucas, J. N. (2000) *Int J Radiat Biol* **76,** 1589-1598.
3. Tawn, E. J., Whitehouse, C. A., Holdsworth, D., Morris, S. & Tarone, R. E. (2000) *Int J Radiat Biol* **76,** 355-65.
4. Whang-Peng, J., Young, R. C., Lee, E. C., Longo, D. L., Schechter, G. P. & DeVita, V. T., Jr. (1988) *Blood* **71,** 403-14.
5. Cornforth, M. N. & Bedford, J. S. (1987) *Radiat Res* **111,** 385-405.
6. Natarajan, A. T. & Zwanenburg, T. S. (1982) *Mutat Res* **95,** 1-6.
7. Brown, J. M., Evans, J. W. & Kovacs, M. S. (1993) *Environ Mol Mutagen* **22,** 218-24.
8. UNSCEAR (2000), New York), pp. 49-72.
9. Durante, M., Cella, L., Furusawa, Y., George, K., Gialanella, G., Grossi, G., Pugliese, M., Saito, M. & Yang, T. C. (1998) *Int J Radiat Biol* **73,** 253-62.
10. Goodhead, D. T. (1992) *Advances in Radiation Biology* **16,** 7-44.
11. Jenner, T. J., deLara, C. M., O'Neill, P. & Stevens, D. L. (1993) *Int J Radiat Biol* **64,** 265-73.
12. Goodhead, D. T. (1999) *Journal of Radiation Research* **40,** 1-13.
13. Savage, J. R. & Simpson, P. J. (1994) *Mutat Res* **312,** 51-60.
14. Griffin, C. S., Marsden, S. J., Stevens, D. L., Simpson, P. & Savage, J. R. (1995) *Int J Radiat Biol* **67,** 431-439.
15. George, K., Wu, H., Willingham, V., Furusawa, Y., Kawata, T. & Cucinotta, F. A. (2001) *Int J Radiat Biol* **77,** 175-183.
16. Grigorova, M., Brand, R., Xiao, Y. & Natarajan, A. T. (1998) *Int J Radiat Biol* **74,** 297-314.
17. Sabatier, L., Al Achkar, W., Hoffschir, F., Luccioni, C. & Dutrillaux, B. (1987) *Mutat Res* **178,** 91-7.
18. Knehr, S., Huber, R., Braselmann, H., Schraube, H. & Bauchinger, M. (1999) *Int J Radiat Biol* **75,** 407-18.
19. Speicher, M. R., Gwyn Ballard, S. & Ward, D. C. (1996) *Nat Genet* **12,** 368-375.
20. Greulich, K. M., Kreja, L., Heinze, B., Rhein, A. P., Weier, H. G., Bruckner, M., Fuchs, P. & Molls, M. (2000) *Mutat Res* **452,** 73-81.
21. Simpson, P. J. & Savage, J. R. (1996) *Int J Radiat Biol* **69,** 429-36.
22. Cornforth, M. N. (2001) *Radiat Res* **155,** 643-59.
23. Loucas, B. D. & Cornforth, M. N. (2001) *Radiat Res* **155,** 660-671.
24. Simpson, P. J., Papworth, D. G. & Savage, J. R. (1999) *Int J Radiat Biol* **75,** 11-8.
25. Sachs, R. K., Chen, A. M., Simpson, P. J., Hlatky, L. R., Hahnfeldt, P. & Savage, J. R. (1999) *Int J Radiat Biol* **75,** 657-672.
26. Goodhead, T. G. (1991) in *Genes, Cancer and Radiation Protection.*, ed. Mendelsohn, M. L. (National Council on Radiation Protection and Measurements., Bethesda, MD.), pp. 25-37.
27. Sachs, R. K., Chen, A. M. & Brenner, D. J. (1997) *Int J Radiat Biol* **71,** 1-19.
28. Rothkamm, K., Kuhne, M., Jeggo, P. A. & Lobrich, M. (2001) *Cancer Res* **61,** 3886-93.

29. Dolling, J. A., Boreham, D. R., Brown, D. L., Raaphorst, G. P. & Mitchel, R. E. (1997) *Int J Radiat Biol* **72,** 303-11.
30. Cremer, C., Munkel, C., Granzow, M., Jauch, A., Dietzel, S., Eils, R., Guan, X. Y., Meltzer, P. S., Trent, J. M., Langowski, J. & Cremer, T. (1996) *Mutat Res* **366,** 97-116.
31. Savage, J. R. (1993) *Environ Mol Mutagen* **22,** 234-44.
32. Savage, J. R. (1993) *Environ Mol Mutagen* **22,** 198-207.
33. Savage, J. R. (2000) *Science* **290,** 62-63.
34. Cremer, T. & Cremer, C. (2001) *Nat Rev Genet* **2,** 292-301.
35. Nikiforova, M. N., Stringer, J. R., Blough, R., Medvedovic, M., Fagin, J. A. & Nikiforov, Y. E. (2000) *Science* **290,** 138-41.
36. Ludwikow, G., Xiao, Y., Hoebe, R. A., Franken, N. A., Darroudi, F., Stap, J., Van Oven, C. H., Van Noorden, C. J. & Aten, J. A. (2002) *Int J Radiat Biol* **78,** 239-47.
37. Chadwick, K. H. & Leenhouts, H. P. (1978) *Int J Radiat Biol Relat Stud Phys Chem Med* **33,** 517-29.
38. Savage, J. R. & Papworth, D. G. (1973) *Mutat Res* **19,** 139-143.

Acknowledgements. We are extremely grateful to John Savage for very useful discussions, advice and many helpful suggestions in the preparation of this manuscript. Similarly, we would like to thank John Thacker for his comments and advice. We are also indebted to David Papworth for performing all the statistical analysis and Anna Bristow, Samantha Marsden, Stuart Townsend and Peter Clapham for technical assistance. This work was supported by the Department of Health, UK. Contracts A2.2/RRX 36 and RRX 95.

Fig. 1. (*A*) Cartoon of a 'complete' α-particle-induced complex given a C/A/B classification of 4/5/6. (*B*) Estimated position of breakpoints on each damaged chromosome. (*C, D* and *E*) Reconstruction of the chromosome 'break-ends' to produce the observed complex. Theoretically, this complex could be produced by the proximate interaction of all 'free-ends' (*C*), thus if no other rejoining solution were possible, this complex would be classified as a 'non-reducible complex of size c6'. However, as shown

in (*D* and *E*), this complex could also be reduced into two different sequential exchanges of sizes (*D*) c2+c4 and (*E*) c3+c3. No other combination of cycles that produced the observed complex were theoretically possible, consequently, the 'Obligate cycle structure' (22) was scored as c3+c3 since this represented the least complex of all theoretical cycle sizes.

Fig. 2. A model was developed to predict the number of chromosome domains crossed by the traversal of a α-particle through the cell nucleus. (*A*) Calculation of number and size of domain intersections in a nuclear equatorial plane (NEP) (*B*) Top view of NEP crossed by 19 parallel chords.

Fig. 3. (*A*) Distribution of the number of chromosome domains that intersect with a NEP (*B*) The mean numbers of domains that are crossed by a single α-particle track in NEPs that are intersected by different numbers of domains.

Fig. 4. Transverse section, at maximum diameter, off modelled peripheral blood lymphocyte (PBL) cell nucleus showing individual chromosome domains being crossed by (*A*) a α-particle and (*B*) electron tracks from two X-ray interactions.

Fig. 5. (*A*) Distribution of the number of domains predicted to be crossed by a single α-track, compared with the distribution of observed number of chromosomes in each complex. Using all α-particle-induced complexes from Table 1A, normalised to model data involving 2 or more domains, a similar trend was seen between the observed number of chromosomes involved in each complex (▲) and that predicted from the model (hashed bar and open bar; open bar being the subset that could be attributed to a track crossing homologous chromosomes). Error bars represent the standard error of the value (assuming a Poisson distribution) (*B*) The number of independent events (simple,

complex or break only) in each damaged cell (▼) was compared to the expected Poisson distribution of nuclei 'hit' by 1,2, 3 or 4 α-particles (Δ), normalised to the single-event cells. Broadbeam irradiation of 0.5Gy delivers a mean of 1 α-particle/cell with a Poisson distribution of particle hits of 51:34:15 for 0:1:>1 particles/nucleus respectively (1). Error bars represent the standard error of the value.

Fig. 6. The proportion of simple and complex aberrations induced after exposure to 0.5 Gy α-particles and 3 Gy X-rays are displayed in two ways. (1) as the number of simple or complex exchanges expressed as a percentage of the 'total exchanges' and (2) as the number of cells containing only simple exchanges or at least one complex exchange, expressed as a percentage of 'all damaged cells'. 32% of cells exposed to α-particles were damaged and 87% of these contained at least one fully definable complex. Considering the cells which did not, we found 1 cell with an exchange classed as a simple, but which contained a 'hidden' complex event, while the remaining 3 cells each showed a single broken chromosome. Such breaks are also observed in sham-irradiated cells and are believed to arise as a consequence of mechanical damage, but they could also be considered as end products of un-rejoined damage to a single chromosome domain. 91% of cells exposed to 3 Gy X-rays were visibly damaged; all contained exchanges.

Fig. 7. (*A*) M-FISH karyotype showing an α-particle-induced complex involving chromosomes 3, 7, 8, 11, 12 and 18 (arrowed) and classified as 6/7/12. (*B*) Details the chromosomes involved and the relative breakpoint positions with each break-end numbered. Based on the breakpoints assigned we can predict completeness of the exchange by assuming either i) chromosomes 7 and 18 have rejoined with themselves (as

shown in *C*) or ii) chromosomes 7 and 18 have exchanged with 18qter and 7qter respectively, but below the limit of resolution (not shown). All other participating chromosome ends of the complex are accounted for but further assumptions for rejoining are required due to the inability to discriminate the orientation of inserted events. In all we can show there are 256 different rejoining paths that are capable of resulting in the visualised complex (data not shown). The scored obligate cycle structure, c2+c3+c3+c4 accounted for less than 1% of all possibilities, while the largest rejoining cycles (c12 (as illustrated in *B*) or c10+c2 or c9+c3) accounted for 77% of all possible rejoining paths (data not shown).

Table 1. Complexity of each independent complex event was assessed according to the minimum number of chromosomes (C) and breaks (B) involved. To prevent ambiguity, we have separated all the data into 3 different sections (*A, B* and *C*). The rationale for this relates to the difficulties faced when classifying complexes when both chromosome homologues are damaged in a cell, illustrated by the finding that only 41% of the complexes in (*A*) were classed as unresolved-incomplete exchanges while 88% and 76% were similarly classed from (*B*) and (*C*). Thus, (*A*) details only those complexes found in cells where no homologous pair was damaged, (*B*) all complexes found in cells that had at least one homologous pair damaged but which were classed as separate events and (*C*) all those remaining complexes that had at least one homologous pair involved in the same event. To address potential mechanistic routes of complex formation we derived every possible theoretical rejoining cycle, based on breakage and reunion, that was capable of resulting in the observed complex. The most conservative or obligate rejoining cycle structure (22) is noted for each complex, the ratio for each cycle in all those showing two

different cycle paths noted is 1:1 except (*) which is 2:1. Considering (*A*), 23/42 complexes were non-reducible (range c2-c6), implying that repair of up to 12 free-ends occurred in the same irreducible interaction, localised in space and possibly time. 2/42 complexes were SECs (c2+c2 and c2+c6) with only one theoretical rejoining path and 17/42 were SECs that had multiple theoretically possible rejoining paths.

Table 1. Complexity of all α-particle-induced complex exchanges

Complexity		A : No homologous pairs		B : Separate-event homologous pairs		C : Same-event homologous pairs	
# chromosomes	# breaks	Total	Obligate cycle structure	Total	Obligate cycle structure	Total	Obligate cycle structure
2	3	5	c3	-	-	2	c3
	4	4	c2+c2 / c4	-	-	-	-
	5	2	c2+c3 / c5	-	-	-	-
3	3	8	c3	-	-	-	-
	4	3	c2+c2 / c4 *	1	c2+c2	2	c2+c2 / c4
	5	1	c5	1	c2+c3	-	-
	6	1	c2+c4	-	-	-	-
	7	1	c2+c2+c3	-	-	-	-
	9	1	c2+c3+c4	-	-	-	-
4	4	1	c4	1	c4	2	c4
	5	2	c2+c3 / c5	1	c5	-	-
	6	2	c3+c3 / c6	1	c3+c3	1	c6
	7	-	-	1	c2+c2+c3	-	-
5	5	-	-	-	-	2	c5
	6	2	c6	-	-	-	-
	7	2	c2+c2+c3 / c3+c4	1	c7	2	c2+c2+c3 / c7
	8	2	c2+c3+c3 / c2+c6	-	-	-	-
	11	1	c2+c2+c3+c4	-	-	-	-
6	9	-	-	1	c3+c3+c3	-	-
	10	2	c2+c3+c5 / c2+c8	-	-	-	-
	11	-	-	-	-	1	c11
	12	1	c2+c3+c3+c4	-	-	-	-
7	9	-	-	-	-	1	c2+c2+c5
	10	1	c2+c3+c5	-	-	-	-
	11	-	-	-	-	1	c11
8	8	-	-	-	-	1	c3+c5
9	11	-	-	-	-	1	c4+c7
10	13	-	-	-	-	1	c13

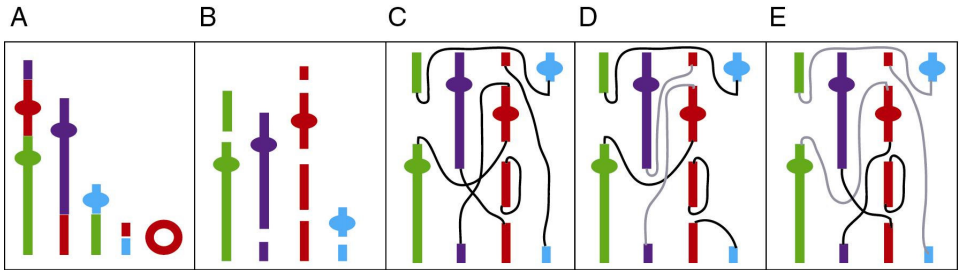
A
B
C
D
E

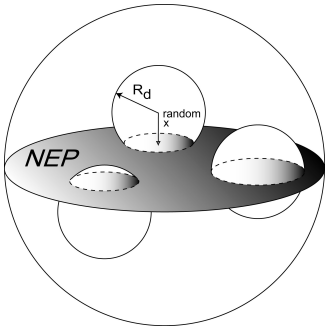
R_d
random
x
NEP

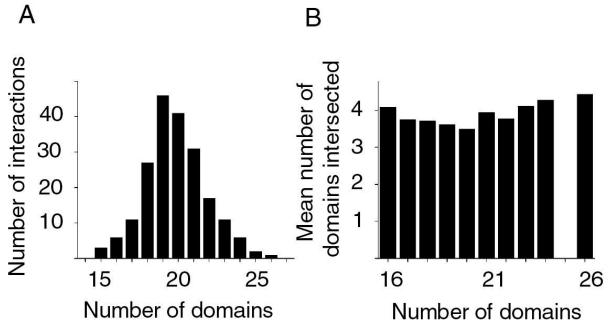
A
B
Number of interactions
40
30
20
10
15
20
25
Number of domains
Mean number of domains intersected
4
3
2
1
16
21
26
Number of domains

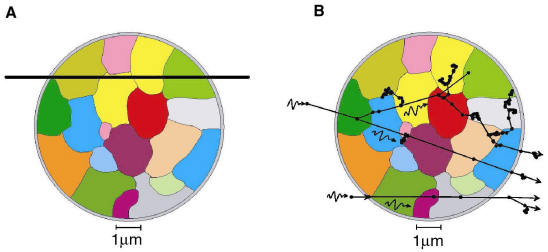
A
B
1μm
1μm

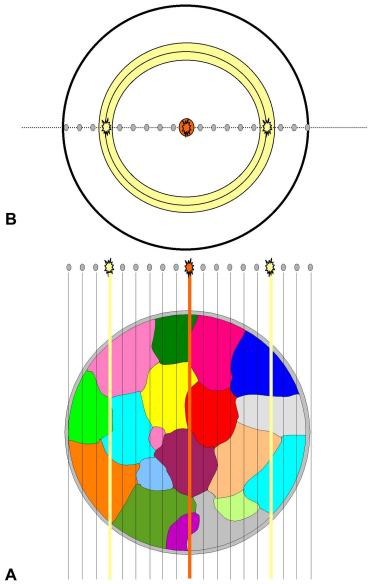
B
A

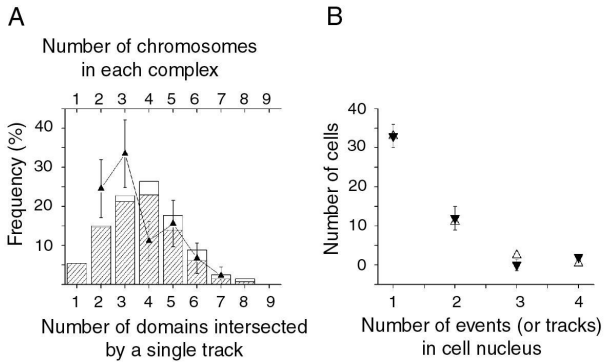
A
Number of chromosomes
in each complex
Frequency (%)
Number of domains intersected
by a single track
B
Number of cells
Number of events (or tracks)
in cell nucleus

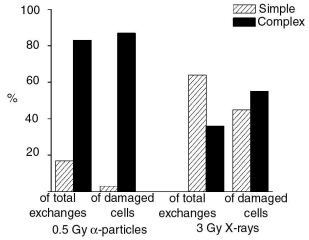
Simple
Complex
%
of total exchanges
of damaged cells
0.5 Gy α-particles
of total exchanges
of damaged cells
3 Gy X-rays

A

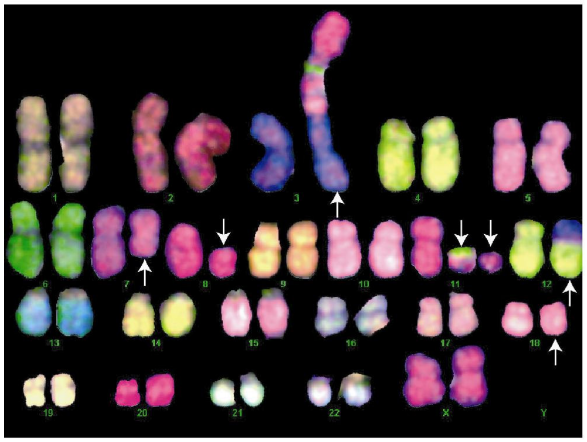

B

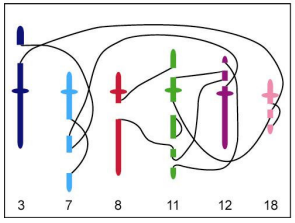

C